Smart Structures and Systems, *Vol. 33, No. 4 (2024) 291-300*
https://doi.org/10.12989/sss.2024.33.4.291

Nonlinear intelligent control systems subjected to earthquakes by fuzzy tracking theory

Z.Y. Chen [1], Y.M. Meng[**1], Ruei-Yuan Wang [1] and Timothy Chen[*1,2]

[1] *Guangdong University of Petrochem Technology, School of Science, Maoming 525000, Peoples Republic of China*
[2] *Division of Engineering and Applied Science, California Institute of Technology, Pasadena, CA 91125, USA*

(*Received August 13, 2022, Revised March 26, 2023, Accepted October 9, 2023*)

Abstract. Uncertainty of the model, system delay and drive dynamics can be considered as normal uncertainties, and the main source of uncertainty in the seismic control system is related to the nature of the simulated seismic error. In this case, optimizing the management strategy for one particular seismic record will not yield the best results for another. In this article, we propose a framework for online management of active structural management systems with seismic uncertainty. For this purpose, the concept of reinforcement learning is used for online optimization of active crowd management software. The controller consists of a differential controller, an unplanned gain ratio, the gain of which is enhanced using an online reinforcement learning algorithm. In addition, the proposed controller includes a dynamic status forecaster to solve the delay problem. To evaluate the performance of the proposed controllers, thousands of ground motion data sets were processed and grouped according to their spectrum using fuzzy clustering techniques with spatial hazard estimation. Finally, the controller is implemented in a laboratory scale configuration and its operation is simulated on a vibration table using cluster location and some actual seismic data. The test results show that the proposed controller effectively withstands strong seismic interference with delay. The goals of this paper are towards access to adequate, safe and affordable housing and basic services, promotion of inclusive and sustainable urbanization and participation, implementation of sustainable and disaster-resilient buildings, sustainable human settlement planning and manage. Simulation results is believed to achieved in the near future by the ongoing development of AI and control theory.

Keywords: damage identification; fuzzy monitoring; Kalman filter; measurement problems; nonlinear hysteresis equation; unknown inputs

1. Introduction

Protecting buildings from natural disasters has always been a major concern in earthquake zones. The main goal of the building management system is to protect the building from external influences such as wind, earthquake and pollution by reducing the vibration transmitted to the building. These methods have been the subject of extensive research in recent years as buildings have become thicker and more flexible. (e.g., Safa 2016, Shariat *et al*. 2018). Especially in system engineering, many methods have been developed to ensure the reliability and performance of non-linear systems. For example, Casciati (1997), Ning *et al*. (2024), Yin *et al*. (2022, 2023), Yu *et al*. (2022), Casciati and Faravelli (2009) and Casciati *et al*. (2014) propose an AI-based approach for engineering applications with non-linear systems.

Structural management methods can be divided into passive, passive and active groups. From conventional isolation systems to adjustable mass dampers (TMD) and liquid column adjustment, passive system dampers use passive elements to dry out vibrations caused by external loads. The semi-active control system, on the other hand, controls the stiffness or stiffness of the system to reduce the vibration caused. Finally, the active structure control system includes actuators that control the behavior of the structure in response to external stimuli. Active structure management systems are well established among structural management systems (Wang *et al*. 2022, 2024, Gao *et al*. 2024, Zhang *et al*. 2023, 2024, Chen *et al*. 2022, 2023a, b).

The main principle of the active antenna array management system is its controller. Over the past two decades, several management algorithms have been used to manage these systems. One of the challenges in designing a functional structure management system is to identify the ambiguity of the uncertainty in forward-looking excitement that implies dynamics. Arrival time delays are another source of uncertainty that may be related to the dynamics of the process, processing time, or network transfer time. Robust control testing is performed in many functional structure control programs, which are common methods for resolving uncertainties. Ballandin and Kogan proposed reliable monitoring of H∞ for seismic resistance of high-rise buildings using linear matrix inequalities. Fuzzy logic control (FLC) is also widely used for active / semi-active control of insecure structural systems due to its robustness.

*Corresponding author,
E-mail: t13929751005@gmail.com
**Co-corresponding author,
E-mail: mengyahui@gdupt.edu.cn

ISSN: 1738-1584 (Print), 1738-1991 (Online)

This controller is ideal for managing building systems where the quality of the building is constantly changing due to the number of occupants and different types of properties. In addition, local damage to structural elements due to external loads can alter the rigidity of the structure. (Dai *et al*. 2023, Deng *et al*. 2024, Xiao *et al*. 2023a, b, c, Xu *et al*. 2022a, b, Du and Wang 2024, Fang *et al*. 2024a, b).

In addition, the H∞ management approach is very useful for building strong management. These hardness parameters can be interpreted in part as H∞ of the transfer function below a given value. This article presents an online management framework for functional structure management systems that simultaneously take into account earthquake uncertainties and time delays. For this purpose, we use the concept of Reinforcement Learning (RL) algorithm for online training of dynamic processors with unplanned controllers. In addition, the proposed controller has a built-in state predictor to calculate the delay time. The control system is implemented in a laboratory scale configuration and its performance is verified through extensive shaker testing under a combination of possible seismic events at a given location.

The rest of the section is organized as follows: First, a structural model and a mathematical model are presented. Control methods and control configurations will be described later. Next, the structure of the seismic fault is considered. Finally, we report and discuss the implementation of control algorithms and test results.

2. Criteria and methods

In this study, the optimal performance of a 10-storey building was considered. The Fig. 1 shows a schematic representation of a structure modeled on a shear frame with 10 degrees of freedom (DOF). Eq. (1) gives the dynamics of motion control of a model in matrix form (Wu *et al*. 2006, Khalatbarisoltani *et al*. 2019)

$$M\ddot{X} + C\dot{X} + KX = -Mr\ddot{x}_g(t) + Du(t)$$
$$C = a_0 M + a_1 K; \quad a_0 = \frac{2\xi W_1 W_3}{W_1 + W_3}; \quad a_1 = \frac{2\xi}{W_1 + W_3}$$
$$M = \begin{bmatrix} m_1 & \cdots & 0 \\ \vdots & \ddots & \vdots \\ 0 & \cdots & m_n \end{bmatrix}; \quad C = \begin{bmatrix} c_1 + c_2 & \cdots & 0 \\ \vdots & \ddots & \vdots \\ 0 & \cdots & c_n \end{bmatrix}; \quad K = \begin{bmatrix} k_1 + k_2 & \cdots & 0 \\ \vdots & \ddots & \vdots \\ 0 & \cdots & k_n \end{bmatrix} \tag{1}$$

where M is the mass matrix, K is the spring matrix, u(t) is the external matrix to control or drive the active energy, r is the voltage coefficient matrix, and D is the control input coefficient matrix. In addition, C is the Rayleigh damping matrix and represents the first and third structural modes, x is the displacement vector and x is the ground velocity later. Using the existing weight, hardness and drying matrices of the model, the equations of motion can be written in the following state spaces

$$x(t) = AX(t) + BU(t) + EF(t);$$
$$A = \begin{bmatrix} 0 & 1 \\ -M^{-1}K & -M^{-1}C \end{bmatrix}_{n*n}; \tag{2}$$
$$B = \begin{bmatrix} 0 \\ M^{-1} \end{bmatrix}_{n*m}; \quad E = \begin{bmatrix} 0 \\ M^{-1} \end{bmatrix}_{n*1}$$

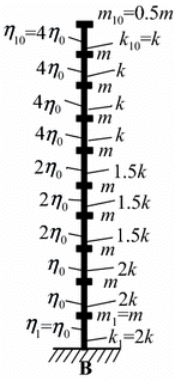

Fig. 1 Schematic representation of a structure modeled on a cross-sectional frame with 10 degrees of freedom (DOF)

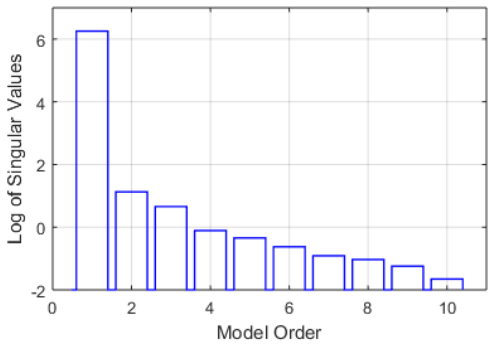

Fig. 2 Hankel singular value estimate for prototype with 10 degrees of freedom

Considering how basic the prototype in this work is reduced to a model with two levels of freedom. The Fig. 2 shows the calculated Hankel singular coefficient of the original model with 10 degrees of freedom. The singular value is a measure of the energy of the corresponding state and its contribution to the process of reaction. As you can see, the individual values assigned to scenarios 1-4 affect the response variables more than any other scenario. This result is consistent with the fact that the fundamental frequency has the greatest influence on the structural variation of the response. Table 2 also shows the natural frequencies of the prototypes. According to Table 2, the third mode is higher than the second. Based on the above considerations, we decided to abandon the third and higher order stages and create a reduced 2DOF version of the original system for on-board testing. A simple system is created with two levels of freedom, the natural frequency and its form corresponding to the original structure. For this, the Rayleigh-Ritz method is used. The test

Table 1 Selected the first five natural frequencies of the sample structure with 10 degrees of freedom

Modal no.	Natural frequency	
	Rad/s	rpm
1	1323.2	12,636
2	1323.2	12,636
3	1649.1	15,748
4	2059.0	19,662
5	2245.1	21,439

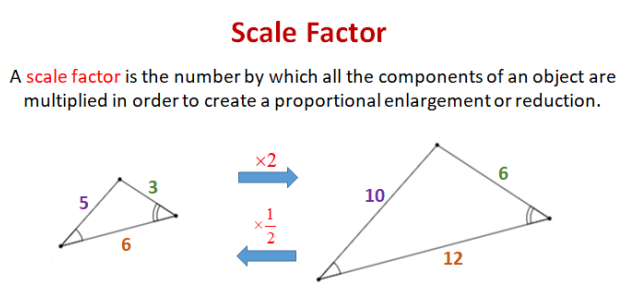

Fig. 3 Reduced model dimensions by the techniques of scale factor description

configuration is based on a simple model. Use the Ibrahim Time Domain (ITD) method to determine the modular parameters of your model, such as natural frequency and waveform. In addition, the integrated test configuration is checked against the test protocol. We compare the eigenfrequencies of the prototype, the simple sample, and the experimental setup. It can be seen that the modular parameters of the experimental configuration are in good agreement with the initial configuration. Fig. 3 shows the experimental setup after a simple procedure.

Eq. (3) shows the equation of motion for this model.

3. Extended Kalman filter based fuzzy theory

On the Figs. 4-5 we will learn how to apply obscure management functions and membership to similar virtual systems. In addition, RL algorithms are methods for autonomous design that are closely related to the environment. Learning reinforcement agents are often advised to approach their good manners with immediate rewards. For example, it is used in some design features of controls.

Learning strategies fall into three categories: controlled learning, uncontrolled learning, and reinforced learning (RL). Artificial neural networks and GAs have been studied in several previous studies in the field of active structure management, but RL, although its properties have not been scaled to a sufficient level for parameter learning. For example, linear artificial neural network controllers and joint controllers of the cerebellar model are common approaches to structural control.

RL algorithms solve problems in which an autonomous agent understands a specific situation from its point of view and performs a specific action to achieve a goal. When an agent acts in nature, he or she is rewarded or punished depending on the action and the circumstances. This article uses the Q-learning algorithm.

We then create dynamic structure management issues as the Markov Decision Process (MDP) for RL systems. MDP is a mathematical model for sequencing decision problems. In this paper, we create a system management problem that acts as MDP, so the RL algorithm with MDP is described by the 5th order (S, A,,, γR T_{xa}). Where S is the order of s. a = $[k_p(m), k_d(n)]$, is a set of obscure rules for the acquisition of a PD controller divided into levels from m = 1 to D and from n = 1 to DD. Except for individual variables, the uncertainty of the model is not considered in this paper T_{xa}. In this case, the controllers are rewarded based on their response to the architecture, so the legal basis of the

$$\begin{bmatrix} x_1 \\ x_2 \\ x_3 \\ x_4 \end{bmatrix} = \begin{bmatrix} 0 & 0 & 1 & 0 \\ 0 & 0 & 0 & 1 \\ \frac{-(k_1+k_2)}{m_1} & \frac{k_2}{m_1} & \frac{-(c_1+c_2)}{m_1} & \frac{c_2}{m_1} \\ \frac{k_2}{m_2} & \frac{-k_2}{m_2} & \frac{c_2}{m_2} & \frac{-c_2}{m_2} \end{bmatrix} \begin{bmatrix} x_1 \\ x_2 \\ x_3 \\ x_4 \end{bmatrix} + \begin{bmatrix} 0 & 0 \\ 0 & 0 \\ -1 & \frac{1}{m_2} \\ -1 & \end{bmatrix} [\ddot{x}_g u(t)], \tag{3}$$

controllers is updated regularly. On the picture. 6 Introduce MDP with current architectural management strategies. In this diagram, they are defined as states or actions.

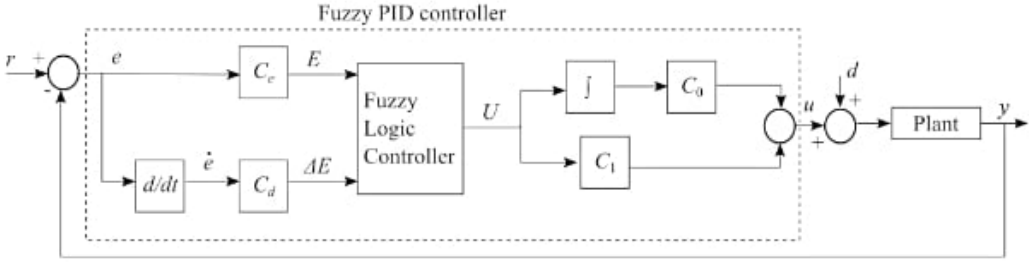

Fig. 4 Controller design for the fuzzy theory

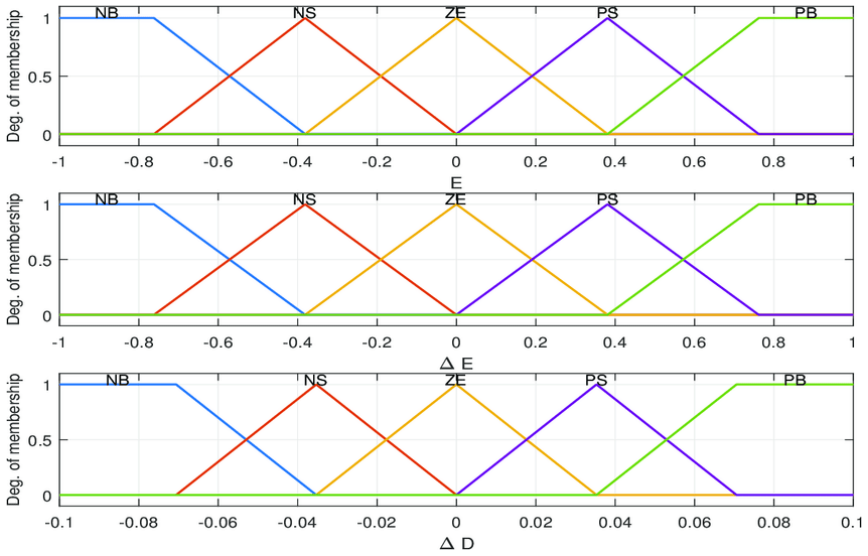

Fig. 5 Inputs and output fuzzy membership functions: (a) displacement of top story; (b) velocity of top story; (c) force

The result of the Q learning algorithm is the Q value, which represents the behavior of the active management system of the structure.

The AQ Q value (s, a) is adjusted periodically according to Eq. (4).

$$Q(s,a) = Q(s,a) + \alpha(r + \gamma\, max_{a' \in A}\, Q\,(s,' a') - Q(s,a)) \tag{4}$$

Where are $\alpha \in [0,1]$ the study rates and $\gamma \in [0,1]$; The reward function is also defined as Eq. (5).

Here, m_i 10 single-axis accelerometers were placed on the ground to evaluate the basic displacement of the main structure analyzed for the volume of the second floor and the corresponding acceleration. $\ddot{x}_i$ The accelerometer can be integrated in accordance with the data of Eq. (6). Base changes are calculated online. Please note that the basic changes calculated in this way may not be very accurate due to differences in the number of people and the type of furniture.

Also α_1, i = 1, ..., 5 is a normal variable. The controller input calculated based on the specification of the PD controller is defined in Eq. (7).

$$R = -1\left(\alpha_1 \frac{|x_{Top}(i)|}{|x_{Top_{max}}|\|_2 \; x_{Top_{max_3}} \frac{|Force(i)|}{|Force_{max}|\|_4 \frac{|\text{Base Shear}(i)|}{|\text{Base Shear}_{max}|\|_5 \frac{|Drift(i)|}{|Drift_{max}|\|}}}}\right) \tag{5}$$

$$\text{Base shear} = \sum_{i=1}^{i=10} m_i\, \ddot{x}_i, \tag{6}$$

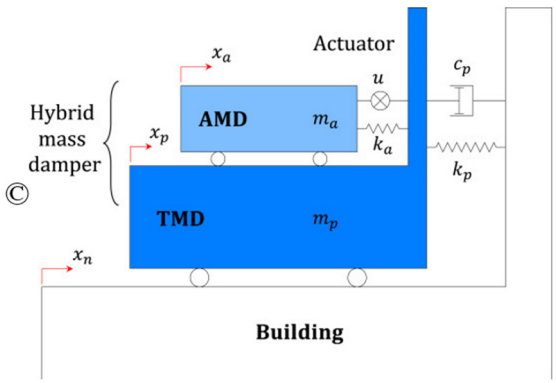

Fig. 6 MDP design criteria for actively managed buildings

$$u(t) = -F_{kp}(x(t) - x_d(t)) - F_{kd}(\dot{x})(t) - \dot{x}_d(t)), \tag{7}$$

Where is also F_{kp} the increase in control set by the controller, maintenance, standby $x(t)$ and F_{kd} the above bias. $x_d(t)$ Desired displacement of the surface layer. Eq. (7) is rewritten as Eq. (8). This allows for zero expected returns, which is a good case for a structured response.

$$u(t) = -F_{kp}x(t) - F_{kd}x(t) \tag{8}$$

Winning rules are calculated by two independent FLCs. Its legal basis is regularly updated with the proposed RL approach. The stability of the dynamic system is estimated by the sign of the eigenvalues of matrix A as follows

$$det(\,sI - A) = s^4 + b_1 s^3 + b_2 s^2 + b_3 s^1 + b_4, \tag{9}$$

Neural networks can be written

$$X(t) = \Psi^S(W^S\Psi^{S-1}(W^{S-1}\Psi^{S-2}(\cdots\cdots\Psi^2(W^2\Psi^1(W^1\Lambda(t)))\cdots\cdots))), \tag{10}$$

Where $\Lambda^T(t) = [X^T(t) \quad U^T(t)]$, as $X^T(t) = [x_1(t) \quad x_2(t) \quad \cdots \quad x_6(t)]$ in the S range, each layer $R^\sigma(\sigma = 1,2,\cdots,S)$ contains neurons and $x_1(t)\sim x_\delta(t)$ is an input variable. $u_1(t)\sim u_m(t)$ Symbolic Weights W^σ Matrix Layer σ^{th} The transfer function vector σ^{th} is defined $\Psi^\sigma(v) = [T(v_1) \quad T(v_2) \quad \cdots \quad T(v_{R^n})]^T$ for this layer.$(\sigma = 1,2,\cdots,S)$.

The NNDI system can be described in state spatial representation (see Bai *et al*. 2021, Cao *et al*. 2023, Hu *et al*. 2023, Li *et al*. 2022, 2023, 2024, Liang *et al*. 2024a, b) as follows

$$Y(t) = A\big(a(t)\big)Y(t),$$
$$A\big(a(t)\big) = \sum_{i=1}^{\gamma} h_\gamma\big(a(t)\big)\bar{A}_i,$$

Where r is a positive integer; is a vector that shows $a(t)$ its dependence on the element $h_i(\cdot)$, i.e., $h_i\big(a(t)\big) = h_i\big(a_1(t),\ a_2(t),\ \cdots,\ a_n(t)\big)$, $a(t) = [a_1(t),\ a_2(t),\ \cdots,\ a_n(t)]^T$ (usually $a(t)$ parallel to the state vector $X(t)$ is $\bar{A}_i(i = 1,2,\cdots,r)$ a fixed matrix $Y(t) = [y_1(t) \quad y_2(t) \quad \cdots \quad y_j(t)]^T$.

By interpolation we get

$$\begin{aligned} X(t) &= \left[\sum_{\varsigma^S=1}^{2} h_{\varsigma^s}(t) G_\varsigma^S\left(W^S\left[\sum_{\varsigma^1=1}^{2} h_{\varsigma^1}(t)\, G_\varsigma^1\big(W^1\Lambda(t)\big)\right]\right)\right] \\ &= \sum_{\varsigma^S-1}^{2}\cdots\sum_{\varsigma^2-1}^{2}\sum_{\varsigma^1-1}^{2} h_{\varsigma^S}(t)\cdots h_{\varsigma^2}(t)h_{\varsigma^1}(t)G_\varsigma^S W^S\cdots G_\varsigma^2 W^2 G_\varsigma^1 W^1\Lambda(t) = \sum_{\Omega^\sigma} h_{\Omega^\sigma}(t)E_{\Omega^\sigma}\Lambda(t) \end{aligned} \tag{11}$$

Where $\sigma = 1,2,\cdots,S,\ \ h_{q_\varsigma^\sigma}(t) \in [0 \quad 1]$,

$\sum_{q_\varsigma^\sigma=1}^{2} h_{q_\varsigma^\sigma}^\sigma(t) = 1;\ \ \varsigma = 1,2,\cdots,R^\sigma;$

$E_{\Omega^\sigma} \equiv G_\varsigma^S W^S\cdots G_\varsigma^2 W^2 G_\varsigma^1 W^1,$

$\sum_{\Omega^\sigma} h_{\Omega^\sigma}(t) \equiv \sum_{\varsigma^S=1}^{2}\cdots\sum_{\varsigma^2=1}^{2}\sum_{\varsigma^1=1}^{2} h_{\varsigma^S}(t)\cdots h_{\varsigma^2}(t)\, h_{\varsigma^1}(t).$

$\sum_{\varsigma^\sigma} h_{\varsigma^\sigma}(t) = \sum_{q_1^\sigma=1}^{2}\sum_{q_2^\sigma=1}^{2}\cdots\sum_{q_R^\sigma{}_\alpha=1}^{2} h_{q_1^\alpha}(t)\, h_{q_2^\alpha}(t)\cdots$

$h_{q_R^\alpha{}_\alpha}(t).$

The dynamics of the NN model can be rewritten as NNDI

$$\dot{X}(t) = \sum_{i=1}^{\gamma} h_i(t)\bar{E}_i\Lambda(t), \tag{12}$$

Where $h_i(t) \geq 0; \sum_{i=1}^{\gamma} h_i(t) = 1;$ r is a positive integer; And $\bar{E}_i$ is a fixed matrix with related dimensions E_{Ω^σ}. The NNDI view can be further restructured as follows

$$\dot{X}(t) = \sum_{i=1}^{\gamma} h_i(t)\{A_i X(t)\}, \tag{13}$$

where A_i These are the parts E_i that match the parts $\Lambda(t)$.

According to the above NN-based system modeling scheme, the nonlinear system can be approximated by the NNDI representation. The NNDI representation follows the same rules as the TS machine learning fuzzy model, combining the flexibility of fuzzy logic theory of machine learning and the rigorous mathematical analysis tools of linear model theory into one model. To test the robustness of the TLP algorithm, we recall the obscure machine learning pattern and TS robust analysis. First, the i-th rule of the TS fuzzy machine learning model, which represents the structural model, can be specified as

$$\begin{aligned} &\text{Me} \quad x_1(t):\cdots \text{Yes}, \quad M_{i1} \text{ yes } x_p(t).M_{ip} \\ &\text{Eat} \quad \dot{x}_j(t) + \sum_{k=1}^{N_j} A_{ikj}x_j(t-\tau_{kj}) + B_{ij}u_j(t) \end{aligned} \tag{14}$$

in which $i = 1,2,\cdots,r$ control numbers; $X(t)$ is the state vector. $M_{ip}(p = 1,2,\cdots,g)$ Fuzzy learning set of $x_1(t)\sim x_p(t)$ variable factor machine.

4. Fuzzy control design

In the following, a stability criterion is proposed to guarantee the asymptotic stability of the nonlinear multiple time-delay large-scale system N. Prior to examination of asymptotic stability, a useful concept is given below.

Lemma 1: For any matrices X and Y with appropriate dimensions, we have $X^TY + Y^TX \leq \xi X^TX + \xi Y^TY$ where ξ is a positive constant.

Theorem 1: The nonlinear multiple time-delay large-scale system N is asymptotically stable, if there exist positive constants $\beta,\ \alpha_j,\ k_j$ and $\rho_j,\ j = 1,2,\cdots,J$ and the feedback gains K_{ij} 's are chosen to satisfy

$$\begin{aligned} &\bar{\lambda}_j = \max_k \lambda_M\big(\bar{Q}_{kj} < 0\big) \ \text{ for } \ k = 1,2,\cdots,N_j \\ &\lambda_{ij} \equiv \lambda_m\big(Q_{ij}\big) > 0 \ \text{ for } \ i = 1,2,\cdots,r_j \\ &\lambda_{ifj} \equiv \lambda_m\big(Q_{ifj}\big) > 0 \ \text{ for } \ i < f \leq r_j \end{aligned}$$

or

$$\Lambda_j = \begin{bmatrix} -\bar{\lambda}_j & 0 & 0 & \cdots & 0 \\ 0 & \lambda_{1j} & \frac{1}{2}\lambda_{12j} & \cdots & \frac{1}{2}\lambda_{1r_jj} \\ 0 & \frac{1}{2}\lambda_{12j} & \lambda_{2j} & \cdots & \frac{1}{2}\lambda_{2r_jj} \\ \vdots & \vdots & \vdots & \ddots & \vdots \\ 0 & \frac{1}{2}\lambda_{1r_jj} & \frac{1}{2}\lambda_{2r_jj} & \cdots & \lambda_{r_jj} \end{bmatrix} > 0$$

Table 2 The variable responds to the actively managed building with no input

(1)	El Centro (assume PGA = 0.l g)		Kobe (assume PGA = 0.l g)	
	Peak (2)	rms (3)	Peak (4)	rms (5)
$x_1(cm)$	3.044	0.843	3.055	1.684
$x_2(cm)$	5.555	1.856	5.466	2.488
$x_3(cm)$	7.265	1.662	6.942	2.749
$\ddot{x}_{1a}(g)$	0.227	0.052	0.223	0.210
$\ddot{x}_{2a}(g)$	0.332	0.057	0.237	0.178
$\ddot{x}_{3a}(g)$	0.361	0.517	0.379	0.213

and $\lambda_M(\bar{Q}_{kj})$ denotes the maximum eigenvalues of $\bar{Q}_{kj}$. Moreover, $\lambda_M(Q_{ij})$ and $\lambda_M(Q_{ifj})$ denote the minimum eigenvalues of Q_{ij} and Q_{ifj}, respectively.

From the robotic system approximation, a nonlinear plant can be viably approximated and portrayed utilizing the automated model including FLC to accomplish the control object.

For $x \in \xi \subset R^n$, $\bar{w} = [\bar{w}_1, \bar{w}_2, \cdots, \bar{w}_n,]^T$ satisfies $\bar{u}(S, \bar{w}) = \bar{w}^T R(S)$ approximated with accuracy ε_{max} over the set ξ so that

$$sup|\bar{u}(S, \bar{w}) - u(S)| \leq \varepsilon_{max} \tag{15}$$

Therefore, the control output could be described as

$$\hat{u}(S, \hat{w}) = \sum_{k=1}^{m} \hat{w}_k \cdot R_k(S) = \hat{w}^T R(S) \tag{16}$$

and then vector $\hat{w}$ of the genetic algorithm needs to be selected with the initial values at time *t* by $\tilde{w} = \bar{w} - \hat{w}$, and then

$$\tilde{w}^T R(S) = \bar{u}(S, \bar{w}) - \hat{u}(S, \hat{w}) \tag{17}$$

$\dot{V} = -\eta \cdot e_m^T Q e_m + 2\eta \cdot S \cdot \left[g(x) \cdot (\tilde{w}^T R(S) + \varepsilon) - 2\eta \cdot |S| \cdot [g(x) \cdot \tilde{w}^T R(S)] \cdot sat\left(\frac{S}{\Phi}\right)\right]$.

When $|S| > \Phi$, then $V \leq -\eta \cdot \|e_m\| \cdot [\|e_m\| \cdot Q - 2\|c\| \cdot \|g(x) \cdot \varepsilon\|]$ with $e_m^T P e_m > \phi^2$.

It is true that $V \leq -\eta \cdot \|e_m\| \cdot \sigma$ if $e_m^T P e_m > \phi^2$ and $|S| > \Phi$, and hence $V < 0$. Thus, V will gradually converge to zero as will all the ζ.

According to the Lyapunov stability theory mentioned above, is guaranteed and the tracking error and the modeling error will then both approach zero.

The Evolved Bat Algorithm (EBA) is proposed as an advanced algorithm to automate global bat selection. Unlike other swarm insight calculations, the real purpose of EBA is that there is only one parameter, called the mean, that must be solved for before using the calculation to solve the problem. Selecting different intermediate objects will determine the bubble size for different scenes during the transition. Air was chosen as the medium in this study because it is the first of many different habitats for turtles. The role of the EBA can be divided into two phases: Implementation: Promulgate the dummy model rather than modify it by ordering as needed. Progression: Fake moves. Generate a random number and check if it is greater than a certain cardiac output. If the result is positive, the pseudo-expert moves with random movements.

$$x_i^f = x_i^{f-1} + D.$$

where x_i^t represents the coordinates of the i-th agent in the t-th iteration and the coordinates of the i-th agent in the last iteration, and D is the distance the agent has moved in this iteration.x_i^{t-1}

$$D = \gamma \cdot \Delta T$$

where γ is the variable associated with the experimentally chosen solution and $\Delta T \in [-1,1]$ is a random number. $\gamma = 0.17$ The medium of choice was air, so we used it in our experiments.

$$x^t{}_i^R = \beta(x_{best} - x_i^t), \beta \in [0,1]$$

where β is a random number. x_{best} We present the closest optimal structures found so far for all organic compounds. Mark the artificial agent's new coordinates after the random walk process is complete.

5. Numerical simulation and results

To demonstrate the implementation of H∞ static control in civil buildings, we performed a detailed numerical simulation using a numerical model of a fully seismic 10-story building. The building is rectangular in shape with an area of 4.5 × 3 meters and a total height of 9 meters (each floor is 3 meters). It is applied on the NCREE vibration table for experimental verification (as shown in Fig. 1). An active gripping system is installed between the first and first floors, which gives the building the strength to withstand earthquakes. The active management structure was tested with LQG management (Huang *et al*. 2021, Jiang *et al*. 2021, Peng *et al*. 2023, Ren *et al*. 2022, Tan *et al*. 2023). A numerical model of the active control structure was successfully proposed, the accuracy of which was confirmed by experimental verification. Therefore, in this article, we use live number modeling as a suitable modeling technique for number simulation. The matrix form of this numerical model can be traced (Shi *et al*. 2023a, b, c, Song *et al*. 2022, Mohammadzadeh *et al*. 2024, Lu *et al*. 2022). This fine model provides relative movement of the ground-related structure for each floor, as well as absolute

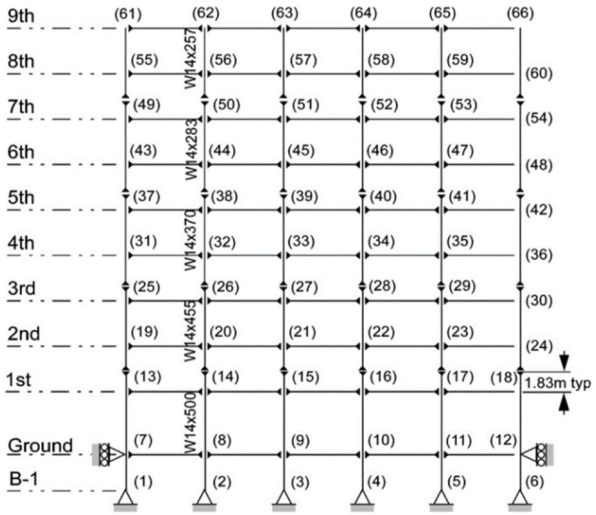

Fig. 7 Values in parentheses indicate percentage reduction compared to free vibration

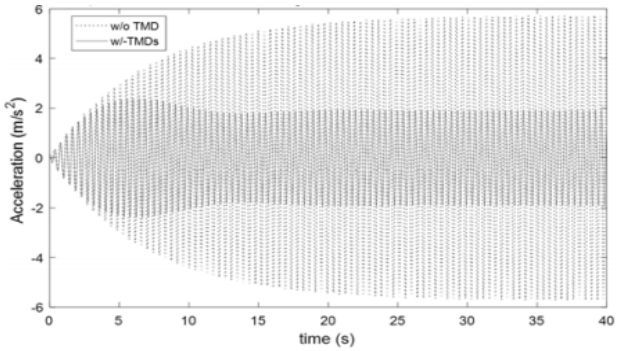

Fig. 8 μ = 0.5% Vertical Peak acceleration by proposed controller subjected to external forces

acceleration for each floor and elevator. The El Centro earthquake in 1940 (100 seconds) and Kobe in 1995 (60 seconds) served as sources of excitement. In this experiment, we used PGA (Peak Ground Acceleration) amplitude obtained at 0.1 g, similar to previous experiments done on the circuit in 2020. It can be easily calculated by multiplying the scale factor.

For comparison, the response of the structure when the earthquake is zero is shown in Table 3. We call this case "out of control". Because the path and speed parameters are expensive, we chose the absolute acceleration of all three phases as the reaction speed. However, the seven return quantities mentioned above are calculated. In phase, the eight state models used by Luo *et al*. 2023a, b, She *et al*. 2023, Zhou *et al*. 2024 to control LQG are derived from another system model constructed using a minimum of state-of-the-art stability and detection accuracy. It should be noted that it was built. A practical approach. To test the reliability of the controller and compare it with the LQG results, this paper uses the same secondary approach to designing a reliable H∞ controller. Here, the difference between secondary and actual performance is taken as the uncertainty of the component, and the chosen weight should include all the limitations on the uncertainty of the component.

We then design H_{∞_1} and H_{∞_2} parameters of two controllers that require small control force and large control force are H_{∞_2} chosen H_{∞_1}, and their simulation results are compared with LOG (small control force) and LOG (large control force). $y = [\ddot{x}_{1a},\ \ddot{x}_{2a},\ \ddot{x}_{3a}]^T$ denotes that unlike proposed controls, the LOG method considers the control function (feedback reduction) as the sole objective of controller design. The weighting functions $W_y = (180\,s + 200)/(1.5\,s + 750)$ and other parameters γ_{min} used in the LMI calculation for H_{∞_1}each H_∞ controller $\alpha = 0.1589, \beta = 0.1589$ are $W_U = (4.4\,s + 200)\,/\,(l\,ls + 440)$: $W_e = (0.02\,s + 21{,}000)/(0.5\,s + 10)$. The

Table 3 Control increases the rate of reduction

Error	RCE						
	HN	MN	SN	ZERO	SP	MP	HP
HN	K_p = dec	K_p = dec	K_p = dec	K_p = dec	K_p = dec	K_p = dec	K_p = dec
	K_i = dec	K_i = med	K_i = inc	K_i = dec	K_i = inc	K_i = med	K_i = dec
MN	K_p = med	K_p = med	K_p = med	K_p = dec	K_p = dec	K_p = dec	K_p = dec
	K_i = med	K_i = med	K_i = inc	K_i = inc	K_i = inc	K_i = inc	K_i = inc
SN	K_p = dec	K_p = dec	K_p = dec	K_p = dec	K_p = dec	K_p = dec	K_p = dec
	K_i = dec	K_i = med	K_i = inc	K_i = med	K_i = inc	K_i = med	K_i = inc
ZERO	K_p = med	K_p = med	K_p = med	K_p = med	K_p = med	K_p = med	K_p = med
	K_i = dec	K_i = med	K_i = inc	K_i = med	K_i = inc	K_i = med	K_i = med
SP	K_p = dec	K_p = inc	K_p = med	K_p = med	K_p = med	K_p = med	K_p = dec
	K_i = dec	K_i = inc	K_i = med	K_i = med	K_i = med	K_i = med	K_i = dec
MP	K_p = med	K_p = inc	K_p = inc	K_p = inc	K_p = inc	K_p = med	K_p = inc
	K_i = dec	K_i = inc	K_i = inc	K_i = dec	K_i = inc	K_i = med	K_i = med
HP	K_p = inc	K_p = inc	K_p = inc	K_p = med	K_p = inc	K_p = inc	K_p = inc
	K_i = dec	K_i = med	K_i = inc	K_i = med	K_i = med	K_i = med	K_i = inc

simulated responses for 0.1 g PGA during the two earthquakes using the H_{∞_1} and H_{∞_2} controls are listed. Values in parentheses in Fig. 7 indicate percentage reduction compared to 'no control' in Table 1 and Fig. 9 with the proposed controller subjected to external forces. From Table 4, we can see that H_{∞_1} control increases the rate of reduction in RMS response. At 50%, the dominant power is approx. Compared to 1000 kgf, the H_{∞_2} controller has increased up to 60%, and the operating force is about 1500 kgf. The reduction in peak response was relatively small, and a significant difference in peak reduction was observed between the two different seismic results. For comparison, the simulated responses by the LQG1 and LQG3 controls are also reported in Table 4. The results show that the proposed H∞ controller provides better performance comparable to the LQG controller in the control frame structure.

6. Conclusions

Analytical solutions of the crosswind closing behavior from a hypothetical self-contained wind system show that the wind parameters are not only a function of wind size and wind speed, but are largely independent of the weight-to-structure reduction ratio. An LMI-based H∞ controller that takes the thickness parameter into account is presented. Robustness criteria include robustness of stability against system uncertainty, and to minimize tracking errors and prevent disturbances and measurement noise. A numerical model of a complete three-story experimental building with an active bracing system is used in simulations to demonstrate that the proposed controller works in a realistic scenario (see Lu *et al*. 2022, Luo *et al*. 2023a, b, Carreras *et al*. 2011 and references therein). Two earthquakes, the El Centro earthquake and the Kobe earthquake, were used in the large-scale simulations. The controller design assumes system uncertainty and for practical reasons the acceleration parameter is used as a feedback quantity. To better demonstrate the potential of the modulation control function in this system, two H∞ controllers were designed.

Additionally, we compare the simulation results of the H∞ controller with the efficiency of the LQG controller. The simulation results show that (1) the LMI method performs well in computing the H∞ controller, and (2) the efficiency of the proposed H∞ controller is remarkable, (3) with the ability to reduce interference, tracking error, and noise. Seeing that the performance of the H∞ controller as efficient as the LQG controller, the proposed robust H∞ control based on LMI is suitable for seismic retrofitting of civil engineering buildings.

References

Adam, T.J. and Horst, P. (2014), "Experimental investigation of the very high cycle fatigue of GFRP (90/0)s cross-ply specimens subjected to high-frequency four-point bending", *Compos Sci Technol*., **101**, 62-70. https://doi.org/10.1016/j.compscitech.2014.06.023

Bai, X., He, Y. and Xu, M. (2021), "Low-thrust reconfiguration strategy and optimization for formation flying using Jordan normal form", *IEEE Transact. Aerosp. Electron. Syst*., **57**(5), 3279-3295. https://doi.org/10.1109/TAES.2021.3074204

Battista, R.C. and Varela, W.D. (2019), "A system of multiple controllers for attenuating the dynamic response of multimode floor structures to human walking", *Smart Struct. Syst*., *Int. J*., **23**(5), 467-478. https://doi.org/10.12989/sss.2019.23.5.467

Bedirhanoglu, I. (2014), "A practical neuro-fuzzy model for estimating modulus of elasticity of concrete", *Struct. Eng. Mech*., *Int. J*., **51**(2), 249-265. https://doi.org/10.12989/sem.2014.51.2.249

Cao, J., Bu, F., Wang, J., Bao, C., Chen, W. and Dai, K. (2023), "Reconstruction of full-field dynamic responses for large-scale structures using optimal sensor placement", *J. Sound Vib.*, **554**, 117693. https://doi.org/10.1016/j.jsv.2023.117693

Carreras, G., Casciati, F., Casciati, S., Isalgue, A., Marzi, A. and Torra, V. (2011), "Fatigue laboratory tests toward the design of SMA portico-braces", *Smart Struct. Syst*., *Int. J*., **7**(1), 41-57. https://doi.org/10.12989/sss.2011.7.1.041

Casciati, F. (1997), "Checking the stability of a fuzzy controller for nonlinear structures", *Comput.-Aided Civil Infrastr. Eng*., **12**, 205-215. https://doi.org/10.1111/0885-9507.00057

Casciati, F and Casciati, S. (2018), "Amelioration and retrofitting of educational buildings", *Earthq. Eng. Eng. Vib*., **17**(1), 47-51. https://doi.org/10.1007/s11803-018-0424-2

Casciati, F. and Faravelli, L. (2009), "A passive control device with SMA components: from the prototype to the model", *Struct. Control Health Monitor*., **16**, 751-765. https://doi.org/10.1002/stc.328

Casciati, F. and Faravelli, L. (2016), "Dynamic transient analysis of systems with material nonlinearity: a model order reduction approach", *Smart Struct. Syst*., *Int. J*., **18**(1), 1-16. https://doi.org/10.12989/SSS.2016.18.1.001

Casciati, F., and Casciati, S. (2016), "Designing the control law on reduced-order models of large structural systems", *Struct. Control Health Monitor*., **23**, 707-718. https://doi.org/10.1002/stc.1805

Casciati, S., Chassiakos, A.G. and Masri, S.F. (2014), "Toward a paradigm for civil structural control", *Smart Struct. Syst*., *Int. J*., **14**(5), 981-1004. https://doi.org/10.12989/sss.2014.14.5.981

Casciati, F., Casciati, S., Elia, L. and Faravelli, L. (2016), "Optimal reduction from an initial sensor deployment along the deck of a cable-stayed bridge", *Smart Struct. Syst*., *Int. J*., **17**(3), 523-539. https://doi.org/10.12989/SSS.2016.17.3.523

Chen, C.W. (2014a), "Interconnected TS fuzzy technique for nonlinear time-delay structural systems", *Nonlinear Dyn*., **76**(1), 13-22. https://doi.org/10.1007/s11071-013-0841-8

Chen, C.W. (2014b), "A criterion of robustness intelligent nonlinear control for multiple time-delay systems based on fuzzy Lyapunov methods", *Nonlinear Dyn*., **76**(1) 23-31. https://doi.org/10.1007/s11071-013-0869-9

Chen, Y., Zhu, L., Hu, Z., Chen, S. and Zheng, X. (2022), "Risk propagation in multilayer heterogeneous network of coupled system of large engineering project", *J. Manage. Eng.*, **38**(3), 4022003. https://doi.org/10.1061/(ASCE)ME.1943-5479.0001022

Chen, F., Zhang, H., Li, Z., Luo, Y., Xiao, X. and Liu, Y. (2023a), "Residual stresses effects on fatigue crack growth behavior of rib-to-deck double-sided welded joints in orthotropic steel decks", *Adv. Struct. Eng.*, **27**(1), 35-50. https://doi.org/10.1177/13694332231213462

Chen, W., Liu, W., Liang, H., Jiang, M. and Dai, Z. (2023b), "Response of storm surge and M2 tide to typhoon speeds along coastal Zhejiang Province", *Ocean Eng.*, **270**, 113646. https://doi.org/10.1016/j.oceaneng.2023.113646

Cheng, B., Wang, M., Zhao, S., Zhai, Z., Zhu, D. and Chen, J. (2017), "Situation-aware dynamic service coordination in an

IoT environment", *IEEE/ACM Transact. Network.*, **25**(4), 2082-2095. https://doi.org/10.1109/TNET.2017.2705239

Claeys, J., Van Wittenberghe, J., De Baets, P. and De Waele, W. (2019), "Characterisation of a resonant bending fatigue test setup for pipes", *Int. J. Sustain. Constr. Des.*, **2**(3), 424-431. https://doi.org/10.21825/scad.v2i3.20541

Dai, Z., Li, X. and Lan, B. (2023), "Three-Dimensional Modeling of Tsunami Waves Triggered by Submarine Landslides Based on the Smoothed Particle Hydrodynamics Method", *J. Marine Sci. Eng.*, **11**(10), 2015. https://doi.org/10.3390/jmse11102015

Deng, E., Wang, Y., Zong, L., Zhang, Z. and Zhang, J. (2024), "Seismic behavior of a novel liftable connection for modular steel buildings: Experimental and numerical studies", *Thin-Wall. Struct.*, **197**, 111563. https://doi.org/10.1016/j.tws.2024.111563

Du, W. and Wang, G. (2014), "Fully probabilistic seismic displacement analysis of spatially distributed slopes using spatially correlated vector intensity measures", *Earthq. Eng. Struct. Dyn.*, **43**(5), 661-679. https://doi.org/10.1002/eqe.2365

Fang, Z., Liang, J., Tan, C., Tian, Q., Pi, D. and Yin, G. (2024a), "Enhancing Robust Driver Assistance Control in Distributed Drive Electric Vehicles through Integrated AFS and DYC Technology", *IEEE Transact. Intell. Vehicl.* https://doi.org/10.1109/TIV.2024.3368050

Fang, Z., Wang, J., Liang, J., Yan, Y., Pi, D., Zhang, H. and Yin, G. (2024b), "Authority allocation strategy for shared steering control considering human-machine mutual trust level", *IEEE Transact. Intell. Vehicl.*, **9**(1), 2002-2015. https://doi.org/10.1109/TIV.2023.3300152

Feng, J., Wang, W. and Zeng, H. (2024), "Integral sliding mode control for a class of nonlinear multiagent systems with multiple time-varying delays", *IEEE Access*, **12**, 10512-10520. https://doi.org/10.1109/ACCESS.2024.3354030

Gao, N., Han, Y., Li, N., Jin, S., & Matthaiou, M. (2024), "When physical layer key generation meets RIS: Opportunities, challenges, and road ahead", *IEEE Wireless Commun.* https://doi.org/10.1109/MWC.013.2200538

Guo, C., Hu, J., Hao, J., Čelikovský, S. and Hu, X. (2023a), "Fixed-time safe tracking control of uncertain high-order nonlinear pure-feedback systems via unified transformation functions", *Kybernetika*, **59**(3), 342-364. https://doi.org/10.14736/kyb-2023-3-0342

Guo, C., Hu, J., Wu, Y. and Čelikovský, S. (2023b), "Non-singular fixed-time tracking control of uncertain nonlinear pure-feedback systems with practical state constraints", *IEEE Transact. Circuits Syst. I: Regular Papers*, **70**(9), 3746-3758. https://doi.org/10.1109/TCSI.2023.3291700

Hu, D., Li, Y., Yang, X., Liang, X., Zhang, K. and Liang, X. (2023), "Experiment and application of NATM tunnel deformation monitoring based on 3D laser scanning", *Struct. Control Health Monitor.*, **2023**, 3341788. https://doi.org/10.1155/2023/3341788

Huang, C., Han, Z., Li, M., Wang, X. and Zhao, W. (2021), "Sentiment evolution with interaction levels in blended learning environments: Using learning analytics and epistemic network analysis", *Austral. J. Edu. Technol.*, **37**(2), 81-95. https://doi.org/10.14742/ajet.6749

Khalatbarisoltani, A., Soleymani, M. and Khodadadi, M. (2019), "Online control of an active seismic system via reinforcement learning", *Struct. Control Health Monit.*, **26**, e2298. https://doi.org/10.1002/stc.2298

Jiang, H., Wang, M., Zhao, P., Xiao, Z. and Dustdar, S. (2021), "A utility-aware general framework with quantifiable privacy preservation for destination prediction in LBSs", *IEEE/ACM Trans. Netw.*, **29**(5), 2228-2241. https://doi.org/10.1109/TNET.2021.3084251

Jiao, B., Qiao, J., Jia, S., Liu, R., Wei, X., Yun, S., Kong, Y., Ye, Y., Du, X., Yu, L. and Cong, B. (2024), "Low Stress TSV Arrays for High-Density Interconnection", *Engineering*. https://doi.org/10.1016/j.eng.2023.11.023

Li, K., Ji, L., Yang, S., Li, H. and Liao, X. (2022), "Couple-group consensus of cooperative–competitive heterogeneous multiagent systems: A fully distributed event-triggered and pinning control method", *IEEE Transact. Cybernet.*, **52**(6), 4907-4915. https://doi.org/10.1109/TCYB.2020.3024551

Li, J., Liu, Y. and Lin, G. (2023), "Implementation of a coupled FEM-SBFEM for soil-structure interaction analysis of large-scale 3D base-isolated nuclear structures", *Comput. Geotech.*, **162**, 105669. https://doi.org/10.1016/j.compgeo.2023.105669

Li, Y., Luo, Y., Wu, X., Shi, Z., Ma, S. and Yang, G. (2024), "Variational Bayesian Learning Based Localization and Channel Reconstruction in RIS-aided Systems", *IEEE Transact. Wireless Commun.* https://doi.org/10.1109/TWC.2024.3380903

Liang, J., Feng, J., Lu, Y., Yin, G., Zhuang, W. and Mao, X. (2024a), "A direct yaw moment control framework through robust TS fuzzy approach considering vehicle stability margin", *IEEE/ASME Transact. Mechatron.*, **29**(1), 166-178. https://doi.org/10.1109/TMECH.2023.3274689

Liang, J., Lu, Y., Wang, F., Feng, J., Pi, D., Yin, G. and Li, Y. (2024b), "ETS-Based Human–Machine Robust Shared Control Design Considering the Network Delays", *IEEE Transact. Automat. Sci. Eng.* https://doi.org/10.1109/TASE.2024.3383094

Liu, Q., Yuan, H., Hamzaoui, R., Su, H., Hou, J. and Yang, H. (2021), "Reduced reference perceptual quality model with application to rate control for video-based point cloud compression", *IEEE Transact. Image Process.*, **30**, 6623-6636. https://doi.org/10.1109/TIP.2021.3096060

Lu, J., Liu, Y., Huang, W., Bi, K., Zhu, Y. and Fan, Q. (2022), "Robust control strategy of gradient magnetic drive for microrobots based on extended state observer", *Cyborg Bionic Syst.* https://doi.org/10.34133/2022/9835014

Luo, R., Peng, Z., Hu, J. and Ghosh, B.K. (2023a), "Adaptive optimal control of affine nonlinear systems via identifier–critic neural network approximation with relaxed PE conditions", *Neural Networks*, **167**, 588-600. https://doi.org/10.1016/j.neunet.2023.08.044

Luo, Y., Liu, X., Chen, F., Zhang, H. and Xiao, X. (2023b), "Numerical simulation on crack–inclusion interaction for rib-to-deck welded joints in orthotropic steel deck", *Metals*, **13**(8), 1402. https://doi.org/10.3390/met13081402

Mohammadzadeh, A., Taghavifar, H., Zhang, C., Alattas, K.A., Liu, J. and Vu, M.T. (2024), "A non-linear fractional-order type-3 fuzzy control for enhanced path-tracking performance of autonomous cars", *IET Control Theory Applicat.*, **18**(1), 40-54. https://doi.org/10.1049/cth2.12538

Ning, Y., Zhu, S., Chu, H., Zou, Q., Zhang, C., Li, J., Xiao, P. and Li, G. (2024), "1-bit Low-Cost Electronically Reconfigurable Reflectarray and Phased Array Based on p-i-n Diodes for Dynamic Beam Scanning", *IEEE Transact. Antennas Propag.*, **72**(2), 2007-2012. https://doi.org/10.1109/TAP.2023.3325650

Peng, T., Zeng, H., Wang, W., Zhang, X. and Liu, X. (2023), "General and less conservative criteria on stability and stabilization of TS fuzzy systems with time-varying delay", *IEEE Transact. Fuzzy Syst.*, **31**(5), 1531-1541. https://doi.org/10.1109/TFUZZ.2022.3204899

Ren, C., Yu, J., Liu, X., Zhang, Z. and Cai, Y. (2022), "Cyclic constitutive equations of rock with coupled damage induced by compaction and cracking", *Int. J. Min. Sci. Technol.*, **32**(5), 1153-1165. https://doi.org/10.1016/j.ijmst.2022.06.010

She, A., Wang, L., Peng, Y. and Li, J. (2023), "Structural reliability analysis based on improved wolf pack algorithm AK-SS", *Structures*, **57**, 105289. https://doi.org/10.1016/j.istruc.2023.105289

Safa, M. (2016), "Potential of adaptive neuro fuzzy inference system for evaluating the factors", *Steel Compos. Struct., Int. J.*,

21(3), 679-688. https://doi.org/10.12989/scs.2016.21.3.679

Shariat, M., Shariati, M., Madadi, A. and Wakil, K. (2018), "Computational Lagrangian Multiplier Method by using optimization", *Steel Compos. Struct., Int. J.*, **29**(2), 243-256. https://doi.org/10.12989/scs.2018.29.2.243

Shi, M., Hu, W., Li, M., Zhang, J., Song, X. and Sun, W. (2023a), "Ensemble regression based on polynomial regression-based decision tree and its application in the in-situ data of tunnel boring machine", *Mech. Syst. Signal Process.*, **188**, 110022. https://doi.org/10.1016/j.ymssp.2022.110022

Shi, Y., Lan, Q., Lan, X., Wu, J., Yang, T. and Wang, B. (2023b), "Robust optimization design of a flying wing using adjoint and uncertainty-based aerodynamic optimization approach", *Struct. Multidiscipl. Optimiz.*, **66**(5), 110. https://doi.org/10.1007/s00158-023-03559-z

Shi, Y., Song, C., Chen, Y., Rao, H. and Yang, T. (2023c), "Complex standard eigenvalue problem derivative computation for laminar–turbulent transition prediction", *AIAA Journal*, **61**(8), 3404-3418. https://doi.org/10.2514/1.J062212

Song, F., Liu, Y., Shen, D., Li, L. and Tan, J. (2022), "Learning control for motion coordination in wafer scanners: toward gain adaptation", *IEEE Transact. Indust. Electron.*, **69**(12), 13428-13438. https://doi.org/10.1109/TIE.2022.3142428

Tan, J., Zhang, K., Li, B. and Wu, A. (2023), "Event-Triggered Sliding Mode Control for Spacecraft Reorientation With Multiple Attitude Constraints", *IEEE Transact. Aerosp. Electron. Syst.*, **59**(5), 6031-6043. https://doi.org/10.1109/TAES.2023.3270391

Tsai, P.W., Hayat, T., Ahmad, B. and Chen, C.W. (2020), "Structural system simulation and control via NN based fuzzy model", *Struct. Eng. Mech., Int. J.*, **56**(3), 385-407. https://doi.org/10.12989/sem.2015.56.3.385

Wang, L., Meng, L., Kang, R., Liu, B., Gu, S., Zhang, Z.,... Ming, A. (2022), "Design and dynamic locomotion control of quadruped robot with perception-less terrain adaptation", *Cyborg Bionic Syst*. https://doi.org/10.34133/2022/9816495

Wang, R., Gu, Q., Lu, S., Tian, J., Yin, Z., Yin, L. and Zheng, W. (2024a), "FI-NPI: Exploring Optimal Control in Parallel Platform Systems", *Electronics*, **13**(7), 1168. https://doi.org/10.3390/electronics13071168

Wang, W., Liang, J., Liu, M., Ding, L. and Zeng, H. (2024b), "Novel Robust Stability Criteria for Lur'e Systems with Time-Varying Delay", *Mathematics*, **12**(4), 583. https://doi.org/10.3390/math12040583

Wu, J.C., Chih, H.H. and Chen, C.H. (2006), "A robust control method for seismic protection of civil frame building", *J. Sound Vib.*, **294**(1-2), 314-328. https://doi.org/10.1016/j.jsv.2005.11.019

Xiao, N., Wang, Y., Chen, L., Wang, G., Wen, Y. and Li, P. (2023a), "Low-frequency dual-driven magnetoelectric antennas with enhanced transmission efficiency and broad bandwidth", *IEEE Antennas Wireless Propag. Lett.*, **22**(1), 34-38. https://doi.org/10.1109/LAWP.2022.3201070

Xiao, Z., Fang, H., Jiang, H., Bai, J., Havyarimana, V., Chen, H. and Jiao, L. (2023b), "Understanding private car aggregation effect via spatio-temporal analysis of trajectory data", *IEEE Transact. Cybernet.*, **53**(4), 2346-2357. https://doi.org/10.1109/TCYB.2021.3117705

Xiao, Z., Li, H., Jiang, H., Li, Y., Alazab, M., Zhu, Y. and Dustdar, S. (2023c), "Predicting urban region heat via learning arrive-stay-leave behaviors of private cars", *IEEE Transact. Intell. Transport. Syst.*, **24**(10), 10843-10856. https://doi.org/10.1109/TITS.2023.3276704

Xu, B. and Guo, Y. (2022), "A novel DVL calibration method based on robust invariant extended Kalman filter", *IEEE Transact. Vehicul. Technol.*, **71**(9), 9422-9434. https://doi.org/10.1109/TVT.2022.3182017

Xu, B., Wang, X., Zhang, J., Guo, Y. and Razzaqi, A.A. (2022a), "A novel adaptive filtering for cooperative localization under compass failure and non-gaussian noise", *IEEE Transact. Vehicul. Technol.*, **71**(4), 3737-3749. https://doi.org/10.1109/TVT.2022.3145095

Xu, J., Park, S.H., Zhang, X. and Hu, J. (2022b), "The improvement of road driving safety guided by visual inattentional blindness", *IEEE Transact. Intell. Transport. Syst.*, **23**(6), 4972-4981. https://doi.org/10.1109/TITS.2020.3044927

Yin, Y., Guo, Y., Su, Q. and Wang, Z. (2022), "Task allocation of multiple unmanned aerial vehicles based on deep transfer reinforcement learning", *Drones*, **6**(8), 215. https://doi.org/10.3390/drones6080215

Yin, H., Wu, Q., Yin, S., Dong, S., Dai, Z. and Soltanian, M.R. (2023), "Predicting mine water inrush accidents based on water level anomalies of borehole groups using long short-term memory and isolation forest", *J. Hydrol.*, **616**, 128813. https://doi.org/10.1016/j.jhydrol.2022.128813

Ying, Z.G., Ni, Y.Q. and Duan, Y.F. (2019), "Stochastic stability control analysis of an inclined stay cable under random and periodic support motion excitations", *Smart Struct. Syst., Int. J.*, **23**(6), 641-651. https://doi.org/10.12989/sss.2019.23.6.641

Yu, J., Dong, X., Li, Q., Lü, J. and Ren, Z. (2022), "Adaptive practical optimal time-varying formation tracking control for disturbed high-order multi-agent systems", *IEEE Transact. Circuits Syst. I: Regular Papers*, **69**(6), 2567-2578. https://doi.org/10.1109/TCSI.2022.3151464

Zhang, H., Xiang, X., Huang, B., Wu, Z. and Chen, H. (2023), "Static homotopy response analysis of structure with random variables of arbitrary distributions by minimizing stochastic residual error", *Comput. Struct.*, **288**, 107153. https://doi.org/10.1016/j.compstruc.2023.107153

Zhang, X., Wang, S., Liu, H., Cui, J., Liu, C. and Meng, X. (2024), "Assessing the impact of inertial load on the buckling behavior of piles with large slenderness ratios in liquefiable deposits", *Soil Dyn. Earthq. Eng.*, **176**, 108322. https://doi.org/10.1016/j.soildyn.2023.108322

Zheng, W., Deng, P., Gui, K. and Wu, X. (2023), "An Abstract Syntax Tree based static fuzzing mutation for vulnerability evolution analysis", *Inform. Software Technol.*, 107194. https://doi.org/10.1016/j.infsof.2023.107194

Zhou, P., Zheng, P., Qi, J., Li, C., Lee, H.Y., Duan, A., Lu, L., Li, Z., Hu, L. and Navarro-Alarcon, D. (2024), "Reactive human–robot collaborative manipulation of deformable linear objects using a new topological latent control model", *Robot. Comput.-Integr. Manuf.*, **88**, 102727. https://doi.org/10.1016/j.rcim.2024.102727